MOLEKUL
eISSN: 2503-0310

Articles
https://doi.org/10.20884/1.jm.2025.20.3.16203

DFT-Based Study of Phenolic-Derived From Nutmeg (*Myristica fragrans*): Promising Bioreductants for Green Synthesis Silver Nanoparticles

Siti Nabila[1], Muhammad Ikhlas Abdjan[2]*, Khusna Arif Rakhman[1]*, Dira Ayu Annisa[1], Ilham S.W. Mauraji[1], Sudir Umar[1]

[1]Department of Chemistry Education, Faculty Teacher Training and Education, Universitas Khairun, Ternate, 97728, Indonesia
[2]Department of Chemistry, Faculty of Mathematics and Natural Sciences, Universitas Negeri Surabaya, Surabaya, 60231, Indonesia

*Corresponding author email: khusna.arif@khairun.ac.id, muhammadabdjan@unesa.ac.id

Received June 11, 2025; **Accepted** November 14, 2025; **Available online** November 20, 2025

ABSTRACT. The manufacture of silver nanoparticles (AgNPs) can be synthesized by reducing silver ions Ag^+ to Ag^0 by a reductant. Nutmeg (*Myristica fragrans*) fruit extract has the potential as a natural reductant (bioreductant) that can donate electrons to reduce Ag^+ as a ligand and capping agent. This study aims to identify the potential of the bioactive compounds in *Myristica fragrans* (Mf) extract for the green synthesis of AgNPs using several parameters, including total energy, HOMO-LUMO, Fukui function, molecular electrostatic potential (MEP), global reactivity, and UV/Vis theoretical spectral analysis. The method used is Density Functional Theory (DFT) with Becke-3-parameter Lee-Yang-Parr (B3LYP) hybrid functionals, using the 6-31G (d,p) basis set for hydrogen (H), carbon (C), oxygen (O) atoms, and the LanL2Dz for the silver (Ag) atom. The results of the study indicate that single bioactive compounds eugenol, chalcone, carvacrol, and terpineol, as well as eugenol-Ag, chalcone-Ag, carvacrol-Ag, and terpineol-Ag complexes, are good reducing agents in the process of reducing Ag^+ ions to Ag^0 as AgNPs. In addition, these phen-Ag complexes show electron excitation at UV/Vis spectrophotometric simulation in the 454-473 nm wavelength range. This study provides a theoretical understanding of Ag^+ reduction by bioactive compounds in Mf extract for green synthesis of AgNPs, thereby providing a scientific basis for developing green methods for eco-friendly, sustainable AgNP synthesis.

Keyword: Bioreductant, DFT, green synthesis, *Myristica fragrans*, silver nanoparticles.

INTRODUCTION

Silver nanoparticles (AgNPs) have attracted much attention because they have unique characteristics, such as antibacterial (Girma et al., 2024), antioxidant (Qubtia et al., 2024), antimicrobial (Shaban et al., 2024), antiviral (Al-Radadi & Abu-Dief, 2024), optical sensor (Liu et al., 2024), and high catalytic ability (Baskaran et al., 2024). The characteristics of AgNPs have been widely applied in various fields, including biomedicine, sensors, photocatalysis (Padmavathi et al., 2024), cosmetics, and agriculture (Rahmah & Hartati, 2023). However, the synthesis of AgNPs still generally relies on hazardous, environmentally unfriendly materials. As an alternative, a green synthesis approach has been developed in chemistry and materials technology (Arain et al., 2024; Batish & Rajput, 2023) by reducing hazardous chemicals using natural materials, such as plant extracts containing secondary metabolite compounds, as bioreductants (Sururi et al., 2025). In addition, secondary metabolite compounds can function as capping agents, stabilizing and preventing the agglomeration of the resulting nanoparticles (Khan et al., 2023; Wirwis & Sadowski, 2023). The green synthesis is considered safer, cheaper, and more sustainable (Batish & Rajput, 2023) than chemical synthesis (Chen et al., 2021).

The ability of bioreductors in the green synthesis of AgNPs is based on the ability of secondary metabolite compounds to reduce Ag^+. These compounds, such as phenolics, flavonoids, and alkaloids, generally contain hydroxyl (-OH), carbonyl (-CO), carboxylate (-COO), and Amine (NH_2) functional groups. Secondary metabolites in natural material extracts can interact with Ag^+ and form an electric double layer to stabilize the particles (Khan et al., 2023). Green synthesis of AgNPs begins with the breakdown of silver nitrate ($AgNO_3$), which is reduced by phenolic compounds, and changes in the group occur. At alkaline pH, the formation of phenolic-Ag complexes (phen-Ag) can accelerate particle growth (Thomas & Thalla, 2023). During the reduction reaction, phenolic compounds donate an electron, reducing Ag^+ to Ag^0 as AgNPs (Heydari & Zaryabi, 2023).

In Indonesia, Mf has excellent potential as a bioreductant in AgNP synthesis due to the availability and abundance of secondary metabolites, such as

alkaloids, flavonoids, terpenoids, phenols, and saponins (Wirwis & Sadowski, 2023). Several phenolic-derived compounds from Mf extract that have bioactive properties and have been successfully isolated are myristicin, safrole, eugenol, methyl eugenol, methyl isoeugenol, and elemicin, which exhibit many pharmacological activities (Elfia & Susilo, 2023). In addition, several bioactive compounds are thought to have potential bioreductant properties (Figure 1), such as eugenol (reported as a significant component in clove extract used for nanoparticle synthesis by Zouaoui et al. [2025]), chalcone, carvacrol (Siegers et al., 2022), and terpineol (Ashokkumar et al., 2022).

Phenolic derivative compounds in **Figure 1** have hydroxyl (-OH) and carbonyl (-CO) functional groups, which can act as bioreductants (Shafi et al., 2025). The methoxy (-OCH_3) and methyl (-CH_3) groups can stabilize Ag^0 as AgNPs through hydrogen-bond interactions (Mikhailova, 2020). In previous studies, a computational approach based on the Density Functional Theory (DFT) method has been widely used to evaluate the reactivity of molecules in complex compounds and metals (Marni et al., 2022).

Several computational and experimental studies have explored the role of plant-derived phenolic compounds in reducing metal ions and stabilizing metal nanoparticles. For instance, DFT-based investigations on catechol (Huang et al., 2016; Usman et al., 2021), quercetin (Aziz et al., 2025), and other phenolic ligands have provided insights into electron transfer mechanisms and the influence of functional groups on Ag^+ reduction and nanoparticle nucleation (Dutta et al., 2024; Trung et al., 2023). However, despite the extensive phytochemical diversity of *Myristica fragrans*, no comprehensive theoretical study has yet described how its major phenolic constituents—such as eugenol, chalcone, carvacrol, and terpineol—interact electronically with Ag^+ ions during nanoparticle formation.

Therefore, this study was conducted theoretically using DFT and TD-DFT to obtain more accurate information on several phenolic derivative compounds in the Mf extract for the green synthesis of AgNPs. The analyzed parameters, which include the Fukui function, molecular electrostatic potential (MEP), global reactivity, and transition state analysis, serve as descriptors to identify the potential of phenolic compounds as bioreductant candidates in the green synthesis of AgNPs.

The limitation of this study is that it is based solely on several quantum chemical parameters of four phenolic compounds, derived from computational studies, to determine the potential of phenolic compounds in the Mf fruit extract as bioreductors in the green synthesis of AgNPs. Therefore, we recommend that it be applied experimentally in the laboratory in the future. The aim is to provide an analysis of the effectiveness of phenolic compounds as reducing agents in the synthesis of AgNPs and to support the theoretical results. In this theoretical study, the interaction between individual phenolic molecules and Ag^+ ions was modeled to represent the initial reduction and nucleation stage of AgNP formation, rather than the entire nanoparticle system. Therefore, this study applies DFT and TD-DFT methods to elucidate the electronic structure, charge-transfer characteristics, and excitation behavior of these compounds, aiming to provide a molecular-level understanding of their potential role as natural bioreductants in the green synthesis of AgNPs. This study is expected to provide comprehensive insight into the development of green synthesis of AgNP.

EXPERIMENTAL SECTION

Structure Preparation

The modeled compounds in this research were phenolic compounds reported in previous research in Mf extracts, such as eugenol (Mosallam et al., 2021), chalcone, carvacrol (Siegers et al., 2022), and terpineol (Ashokkumar et al., 2022). Then, the complex structure with Ag atoms was modeled to understand their chemical behavior. In this work, a single Ag atom was used as a representative model to simulate the initial interaction between Ag^+ ions and phenolic ligands. This simplified approach allows analysis of the fundamental charge-transfer mechanism and the electronic behavior that precedes the nucleation of silver nanoparticles. The validity of this simplified model is supported by the consistency between the calculated excitation wavelengths (454–473 nm) and the experimental surface plasmon resonance (SPR) range of AgNPs (400–500 nm). The modeled compounds were constructed and optimized by using the Becke-3-parameter Lee-Yang-Parr (B3LYP) hybrid function using the 6-31G (d,p) basis set for hydrogen (H), carbon (C), and oxygen (O) atoms and LanL2Dz silver (Ag) atom through Gaussian 09W software (Pranowo et al., 2018). The B3LYP functional with the 6-31G(d,p)/LANL2DZ basis set was chosen because it provides a reliable balance between computational efficiency and accuracy for organic–metal systems. This level of theory has been widely validated in previous DFT and TD-DFT studies of silver–ligand complexes, showing good agreement with experimental results.

The geometry optimization was performed in the gas phase without applying any implicit solvent model. The default Gaussian convergence criteria were employed, ensuring the energy gradient and displacement thresholds were below 10^{-6} Hartree and 10^{-3} Å, respectively. Dispersion correction (Grimme's D3) was not applied, as the primary purpose of this study was to compare the relative reactivity trends among phenolic derivatives rather than to obtain highly accurate absolute interaction energies. This step aims to get the optimized structure corresponding to the ground-state minimum energy in the ground state.

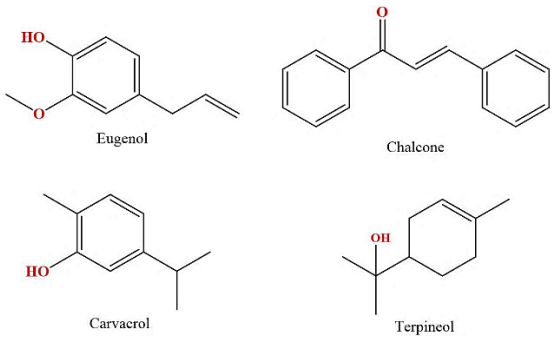

Figure 1. Examples of bioactive compounds acting as reductants

Quantum-Chemical Properties

Quantum-chemical properties were calculated using the Fukui function, MEP, and global reactivity. The calculated quantum parameters, including the HOMO–LUMO gap, Fukui functions, MEP, and global reactivity indices, were used to evaluate the electron-donating ability, reactive sites, and overall charge-transfer tendency of the compounds toward Ag^+ ions. These descriptors collectively provide theoretical insight into the reduction mechanism and stability of AgNP formation. Fukui function analysis to identify molecular sites that can interact as electrophilic (f_x^-) and nucleophilic (f_x^+), which can be calculated using equations (Eqn. 1) and (Eqn. 2).

$$(f_x^-) = Q_x(N) - Q_x(N\text{-}1) \quad (1)$$

$$(f_x^+) = Q_x(N) - Q_x(N+1) \quad (2)$$

$$\Delta f_x = f_x^+ - f_x^- \quad (3)$$

The partial charge of each atom (x) in the molecule is expressed in the variable Q, where $Q_x(N)$ represents the neutral molecule, $Q_x(N\text{-}1)$ the cation, and $Q_x(N+1)$ the anion (Sakr et al., 2022). The Δf_x (Eqn. 3) is an indicator of determining the electrophilic and nucleophilic properties of an atom. The $\Delta f_x > 0$ is electrophilic, and $\Delta f_x < 0$ is nucleophilic. MEP was analyzed through the gap energy from the difference between HOMO and LUMO (Eqn. 4). The HOMO, as the highest occupied molecular orbital, and the LUMO, as the lowest unoccupied molecular orbital, can serve as key references for studying molecular reactivity (Ojha et al., 2023). Several global reactivity descriptor parameters, such as electronegativity/x (Eqn. 5), chemical hardness/η (Eqn. 6), chemical potential/μ (Eqn. 7), global softness/s (Eqn. 8), and electrophilicity index/ω (Eqn. 9), can be calculated using the following equation (Abdjan et al., 2023):

$$\Delta EG = E_{HOMO} - E_{LOMO} \quad (4)$$

$$x = -\frac{1}{2}(E_{HOMO} - E_{LOMO}) \quad (5)$$

$$\eta = \frac{1}{2}(E_{HOMO} - E_{LOMO}) \quad (6)$$

$$\mu = -x \quad (7)$$

$$s = \frac{1}{2}\eta \quad (8)$$

$$\omega = \mu^2/2\eta \quad (9)$$

Transition State Analysis

Transition-state analysis was performed using TD-DFT with the B3LYP hybrid functional and the LanL2DZ basis set for each complex. The parameters described are wavelength (nm), energy gap (eV), oscillator strength (f_0), orbital contribution (%), and transition type. The analyzed parameters in this step aim to understand the electron behavior when it has been promoted to a higher energy level compared to the ground state.

RESULTS AND DISCUSSION

The bioactive compounds of Mf extract, eugenol, carvacrol, chalcone, terpineol, and eugenol-Ag, chalcone-Ag, carvacrol-Ag, and terpineol-Ag complexes were modeled in 3D (**Figure 2**) and optimized for total energy (Et), HOMO-LUMO, and dipole moment.

Complex compounds of Ag and phenolic-derived compounds as electron donors were constructed by coordination covalent bonds, where ligands of phenolic-derived compounds donate free electron pairs to Ag^+ to form stable molecules and are claimed as AgNP (Handayani et al., 2021). In the complexes of phen-Ag for eugenol, chalcone, carvacrol, and terpineol, electrons are donated from the hydroxyl functional group (-OH). Meanwhile, the Ag^+ ion has unfilled orbitals that can accept electrons. Reduction mechanism scheme of complex compounds eugenol-Ag, chalcone-Ag, carvacrol-Ag, and terpineol-Ag, as shown in the chemical reactions (1) to (4).

$$C_{10}H_{12}O_2 + Ag^+ \xrightarrow{OH^-} [C_{10}H_{11}O\text{-}Ag] + H^+ \quad (1)$$

$$C_{10}H_{14}O + Ag^+ \xrightarrow{OH^-} [C_{10}H_{13}O\text{-}Ag] + H^+ \quad (2)$$

$$C_{15}H_{12}O + Ag^+ \xrightarrow{OH^-} [C_{15}H_{12}O\text{-}Ag] + H^+ \quad (3)$$

$$C_{10}H_{18}O + Ag^+ \xrightarrow{OH^-} [C_{10}H_{17}O\text{-}Ag] + H^+ \quad (4)$$

Geometry Optimization

The optimized geometries of the molecular structures of single phenolic-derived and complex compounds have total energies, as shown in **Table 1**. In green synthesis of AgNPs, total energy is an important factor in determining the optimal structure based on the lowest energy state (Evita et al., 2022). The compounds with higher total energy are more unstable and easier to interact with other atoms. Meanwhile, in the formation of complex compounds, the total energy decreases or remains low, indicating that this compound has interactions in the complex that have stronger interatomic attractions, weaker interatomic repulsions, and a more stable complex

conformation (Silfadani et al., 2022). The HOMO energy shows the donating electrons' ability, while the LUMO energy as the acceptor electrons (Rakhman, et al., 2020).

According to **Table 1**, carvacrol and terpineol have higher total energy and are relatively unstable. In contrast, eugenol and chalcone are more stable because they have lower total energies and readily donate electrons to Ag^+ ions to form AgNPs. It can also be seen based on the HOMO-LUMO energy (**Figure 3**), where the chalcone compound has a high HOMO energy so that electrons are excited to the LUMO orbital and can form a stable chalcone-Ag complex.

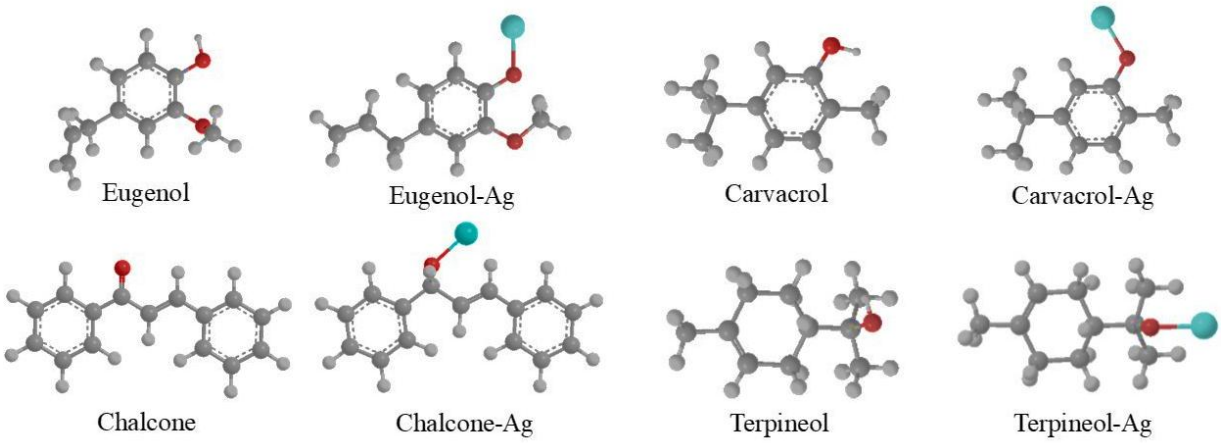

Figure 2. 3D image of phenolic-derived compounds and phen-Ag complexes

Table 1. Geometry optimization data: total energy, HOMO, LUMO, and dipole moment

Compounds	Total energy (kcal/mol)	E_{HOMO} (eV)	E_{LUMO} (eV)	Dipole moment (D)
Eugenol	-338.004	-5.7250	0.0604	22.108
Chalcone	-410.093	-6.3212	-2.1116	3.0039
Carvacrol	-291.636	-5.7263	0.2391	1.4213
Terpineol	-293.139	-5.9772	1.1058	1.5311
Eugenol-Ag	-429.072	-4.8101	-3.6928	6.8093
Chalcone-Ag	-502.189	-5.8474	-3.1638	4.9158
Carvacrol-Ag	-382.668	-4.9728	-3.5766	5.4619
Terpineol-Ag	-384.165	-5.8071	-3.0912	3.6400

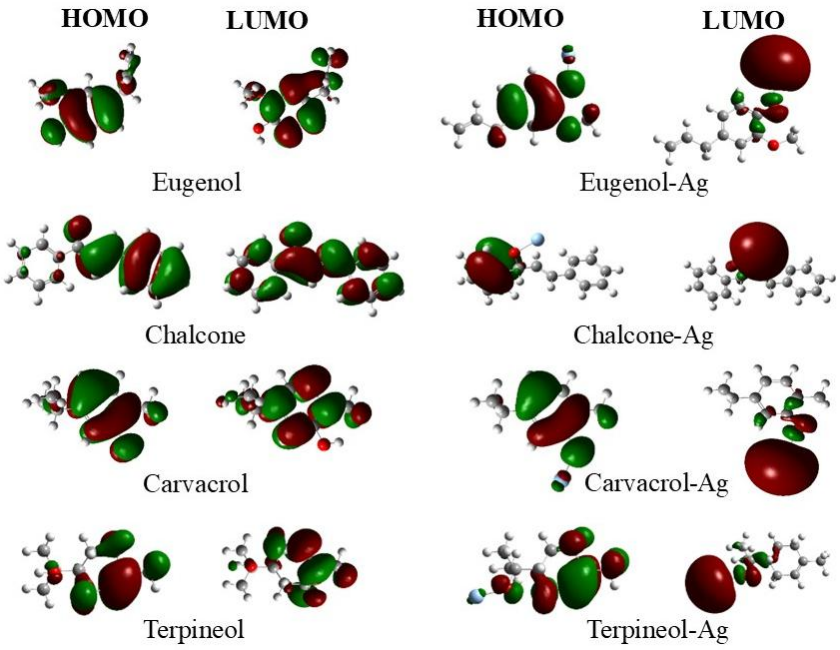

Figure 3. Visualization of energy HOMO-LUMO bioactive and complex compounds

Complexes of eugenol-Ag and chalcone-Ag are also characterized by a decrease in the total energy from their single compounds. The decrease in total energy indicates an increase in AgNP stability. Meanwhile, the eugenol-Ag complex has a higher HOMO energy than others, facilitating easier electron excitation to the LUMO and a faster reduction to produce AgNP. It has also been reported that the higher the HOMO energy, the stronger the organic molecules are attached to metal ions as a complex (Rakhman, Saraha, et al., 2020).

The dipole moment describes the distribution of molecular charges in the green synthesis of AgNP and affects the ability of phenolic compounds to interact with metal surfaces (Akrom, 2022). The dipole moment is determined by the distance between the centers of the positive and negative charges, indicating an uneven distribution of charge in the molecule. High dipole moments exhibit greater polar character, with reactive negative charges that can attract metal cations via coordination bonds. Therefore, compounds with high dipole moments tend to be reactive in the AgNP form process (Putro et al., 2024). In **Table 1**, eugenol and chalcone are more polar and exhibit higher dipole moments with uneven charge distributions, so they can interact with Ag^+ and reduce to Ag^0 to form stable AgNPs.

Chemical Quantum Parameters

The nature of the electronic structure and reactivity tendencies of bioactive compounds, as reflected in Fukui functions, MEPs, and global reactivity, needs to be reviewed to explain the green synthesis of AgNPs theoretically. Global reactivity shows the ability of a molecule to interact both as an electrophile and a nucleophile, which can be determined by several parameters such as energy gap (ΔE_g), electronegativity (x), chemical potential (μ), global hardness (η), global softness (s), and electrophilic index (ω), which are presented in **Table 2**.

In **Table 2**, ΔE_g informs a molecule that experiences electron excitation to a higher orbital. The small ΔE_g easily electron excitation from the HOMO to the LUMO energy levels. Conversely, the large ΔE_g indicates that electron excitation does not occur, and the compounds are stable (Agustina & Kasmui, 2021). In complex formation, a decreasing ΔE_g indicates a strong interaction between bioactive compounds and metal ions, which is important information for AgNP formation (Hussain et al., 2020). Chalcone shows the smallest ΔE_g (**Table 2**) compared to other compounds. Therefore, chalcone compounds are highly reactive because electrons are readily excited from the HOMO to the LUMO, and they are effective for AgNP formation, suggesting that their π-conjugated systems enable effective electron delocalization, thereby enhancing their reducing ability. This finding is also consistent with the high electronegativity value observed for the chalcone–Ag complex, indicating an increased tendency to attract and transfer electrons toward Ag^+ ions. The eugenol-Ag, chalcone-Ag, and carvacrol-Ag compound complexes showed a significant ΔE_g decrease after binding Ag^+ ions, thus confirming the formation of AgNP. The electronegativity of chalcone increases upon complexation with Ag+, indicating that it acts as an electron donor to Ag^+ ions. High electronegativity suggests that electrons are transferred towards the metal surface (Raj et al., 2020). However, in complex compounds, enhanced electronegativity indicates greater ability to stabilize negative charges, thereby reducing Ag^+ ions to AgNPs.

Furthermore, the reduction ability can be explained in terms of molecular orbital interactions. The HOMO orbitals of phenolic derivatives, primarily localized on oxygen atoms and π-bonded aromatic regions, serve as the main electron donors. Upon coordination with Ag^+, these HOMO orbitals overlap with the vacant orbitals of Ag, promoting charge transfer and stabilization through the formation of Ag–O bonds. This charge-transfer mechanism aligns with the results of the Fukui function and MEP analyses, which both highlight the oxygen atoms of hydroxyl and carbonyl groups as dominant nucleophilic sites with high electron density. The red regions in the MEP maps (**Figure 4**) correspond to these donor sites, confirming that the electron-rich oxygen atoms are responsible for Ag^+ reduction. Therefore, the observed decrease in ΔE_g and the increase in electronegativity upon complex

Table 2. Energy gap, electronegativity, global hardness, global softness, chemical potential, and electrophilic index

Compounds	Parameters					
	ΔEg	(x)	(μ)	(η)	(s)	(ω)
Eugenol	5.7854	2.8322	-2.8322	2.8927	1.4463	1.3865
Chalcone	4.2096	4.2164	-4.2164	2.1048	1.0524	4.2232
Carvacrol	5.9655	2.7435	-2.7435	2.9827	1.4913	1.2617
Terpineol	7.0831	2.4356	-2.4356	3.5415	1.7707	0.8375
Eugenol-Ag	1.1173	4.2515	-4.2515	0.5586	0.2793	16.1776
Chalcone-Ag	2.6835	4.5056	-4.5056	1.3417	0.6708	7.5648
Carvacrol-Ag	1.3962	4.2747	-4.2747	0.6981	0.3490	13.0880
Terpineol-Ag	2.7159	4.4491	-4.4491	1.3579	0.6789	7.2885

Table 3. Fukui function of bioactive compounds

Compounds	Position	f_x^+	f_x^-	Δf_x
Eugenol	1-O	0.33	0.38	-0.05
	2-O	0.46	0.32	0.14
Chalcone	16=O	-0.09	0.09	-0.18
Carvacrol	11-O	-0.16	0.07	-0.23
Terpineol	1-O	-0.11	0.11	-0.22

Note: The calculation was performed for the oxygen atom for each group function of the modelled compound.

formation can be attributed to enhanced orbital interaction and electron delocalization between phenolic ligands and Ag^+ ions. These synergistic effects rationalize the efficient bioreduction of eugenol, chalcone, and carvacrol, supporting the proposed theoretical mechanism of AgNP formation.

The global hardness represents the resistance of molecules to electron transfer, while global softness indicates their ability to accept charges. The low global hardness and high global softness indicate that the molecule was more reactive and easier to interact with the metal ions (Akrom & Sutojo, 2023). The lowest global hardness is shown in 2.1048 eV by chalcone, while the highest global softness is in 1.7707 eV by terpineol. The eugenol-Ag has the lowest global hardness of 0.5586 eV, indicating that electron transfer from bioactive compounds to Ag^+ ions in the AgNP form is easy.

Fukui function analysis shows the active site of a molecule that can interact as a nucleophile (f_x^+) and an electrophile (f_x^-). Meanwhile, the Δfx indicates the electrophilic and nucleophilic characteristics. If $\Delta f_x > 0$ is electrophilic and $\Delta f_x < 0$ is nucleophilic, as presented in **Table 3**.

Table 3 presents the position of atoms in bioactive molecules as nucleophiles or electron donors, including eugenol (OH and OCH_3), chalcone (C=O), carvacrol (OH), and terpineol (OH). Donor atoms will reduce Ag^+ to form AgNP. Overall, hydroxyl and ketone groups in each modeled structure indicate a nucleophilic site. In contrast, the methoxy group is indicated as an electrophilic site. These findings indicate that the higher site possibility will interact with AgNPs. Briefly, the hydroxyl group may contribute more to the formation of the phenolic-Ag complex. This result is also supported by the MEP surface visualization (**Figure 4**). It can describe molecular size, electronegativity, shape, and atomic charge density (Dhifet et al., 2025). The MEP simulations allow the electrostatic potential of a molecule to be shown with a color gradient, as shown in Figure 4. Red indicates negative, which is nucleophilic, blue indicates positive, which is electrophilic, and green indicates neutral. Furthermore, **Figure 4** shows a high electron density or negative charge around the donor oxygen atom (red-orange) (Chatterjee et al., 2024), while the electron acceptor region is around Ag (blue). MEP confirms the complex formation with O-Ag interactions on each phenolic derivative group in forming AgNP. According to the data, the correlation of Fukui function and MEP parameters shows a good correlation that describes the hydroxyl group as a nucleophilic site and holds the primary site interaction with the Ag atom.

Transition State Analysis

The energy gap is correlated with the UV/Vis spectrum and can be simulated using TD-DFT/B3LYP/LanL2DZ, as shown in **Figure 5**. The UV-Vis spectrum shows the interaction of molecules with electromagnetic waves in the UV/Vis area and driving electronic transitions in the HOMO and LUMO levels. The simulation UV/Vis spectrum parameters, including wavelength (nm), energy gap (eV), oscillator strength (f_0), and transition type, are presented in **Table 4**.

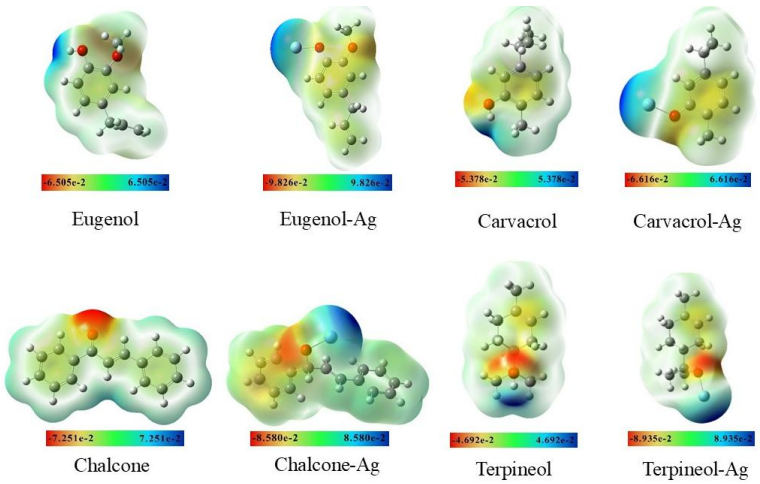

Figure 4. MEP surface analysis of phenolic-derived and complexes

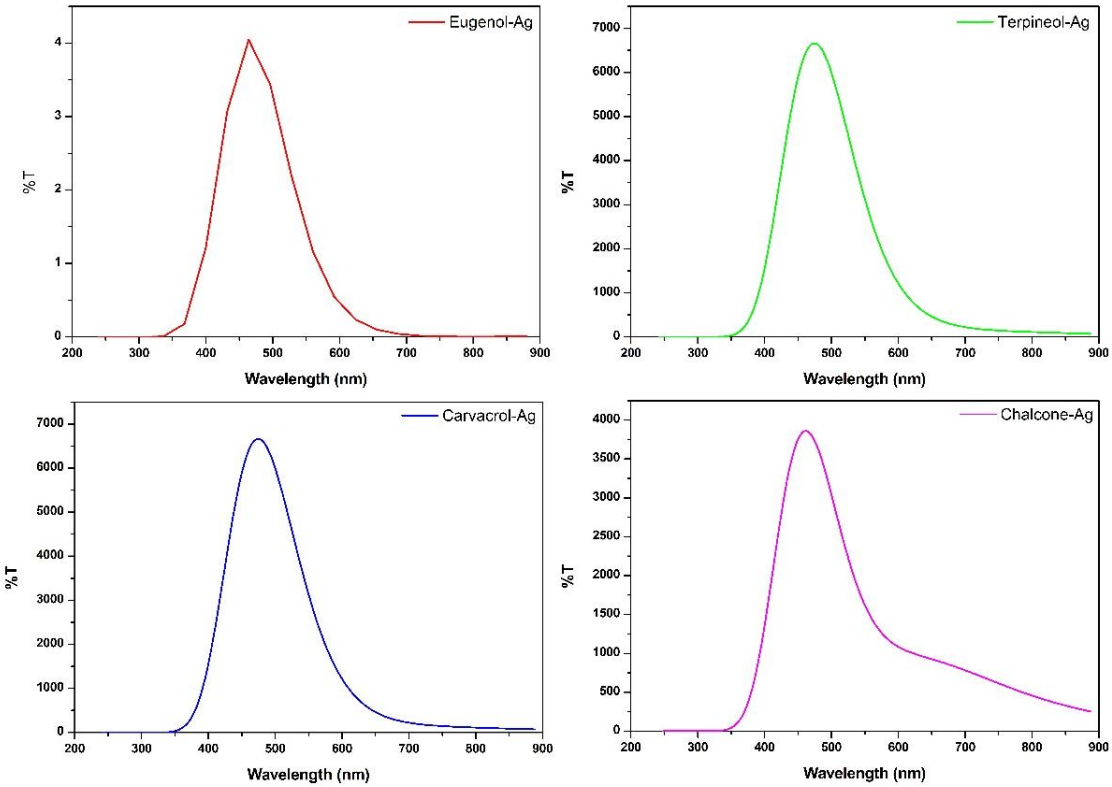

Figure 5. UV/Vis spectra of complexes phen-Ag

Table 4. The excitation energy, oscillator strength, band gap, and transition

Complexes	Excitation energy (nm)	Band gap energy (Ev)	Oscillator strength (f_0)	Transition
Eugenol-Ag	465	1.1173	0.0001	n → π*
Chalcone-Ag	460	2.6835	0.0946	π → π*
Carvacrol-Ag	454	1.3962	0.1316	π → π*
Terpineol-Ag	473	2.7159	0.1607	n → σ*

Experimentally, the formation of AgNPs shows a peak in the visible spectrum at 400-500 nm (Rana & Chowdhury, 2020), a unique characteristic of SPR materials (Juma et al., 2024; Kaur et al., 2020). Three phenolic derivative compounds from Mf extract showed SPR peaks, emphasizing the role of eugenol, carvacrol, and terpineol as bioreductors in the green synthesis of AgNP.

Table 4 shows the results of SPR peak identification on three eugenol-Ag complex compounds at 465 nm, chalcone-Ag at 460 nm, carvacrol-Ag at 454 nm, and terpineol-Ag at 473 nm, with F_0, respectively, $1{\cdot}10^{-4}$, $9.4{\cdot}10^{-2}$, $1.3{\cdot}10^{-1}$, and $1.6{\cdot}10^{-1}$, which are in good agreement with this experimental SPR range. This correspondence confirms that the simulated electronic transitions are responsible for the characteristic plasmonic behavior of AgNPs, indicating the successful theoretical modeling of Ag^+ reduction into metallic Ag^0.

In the UV/Vis spectrum, f_0 corresponds to the absorption intensity (Dhifet et al., 2025). The absorption of the resulting complex is caused by the transition of the π bond orbital (HOMO) to π* (LUMO) for chalcone-Ag and carvacrol-Ag complexes. In addition, there are also n to π* and n to σ* transitions originating from nonbonding electron pairs for the eugenol-Ag and terpineol-Ag complexes. These transitions correspond to ligand-to-metal charge transfer (LMCT) processes, which play a crucial role in initiating the reduction of Ag^+ to Ag^0.

Overall, the TD-DFT results demonstrate that both types of transitions—π→π* and n→π*/n→σ*—contribute cooperatively to the bioreduction mechanism. The π→π* transitions promote delocalized charge movement across the aromatic system, while n→π*/n→σ* transitions enable electron transfer from oxygen donors to Ag^+. These electronic excitations not only explain the calculated absorption in the SPR region but also rationalize the theoretical mechanism of AgNP stabilization and growth in the green synthesis process.

CONCLUSIONS

Bioactive compounds of Mf extract, eugenol, chalcone, carvacrol, and terpineol, as well as eugenol-Ag, chalcone-Ag, carvacrol-Ag, and terpineol-Ag

complexes, have been successfully studied theoretically by DFT and TD-DFT using several parameters such as Fukui function, MEP, global reactivity, and UV/Vis spectrum in green synthesis of AgNP. The results of the Fukui function study show that eugenol, chalcone, carvacrol, and terpineol have the potential as bioreductors in green synthesis of AgNP, due to the presence of oxygen and hydroxyl groups as candidate electron donors. The MEP showed that eugenol-Ag, chalcone-Ag, carvacrol-Ag, and terpineol-Ag were successfully mapped as complexes with dynamic electron transfer at the oxygen atom on the hydroxyl group. Meanwhile, the UV/Vis spectra study provides information on electronic excitation in the HOMO-LUMO orbitals of eugenol-Ag, chalcone-Ag, carvacrol-Ag, and terpineol-Ag through the formation of SPR peaks, a unique characteristic of AgNPs, which show a wavelength peak in the 400-500 nm range.

ACKNOWLEDGEMENTS

The authors would like to thank LPPM and FKIP Universitas Khairun for funding this research through the PKUPT FKIP 2025 program (Project No. 006/PEN-PKUPT/PG.12/2025). The financial support provided was essential for the successful completion of this study.

REFERENCES

Abdjan, M. I., Aminah, N. S., Kristanti, A. N., Siswanto, I., Saputra, M. A., & Takaya, Y. (2023). Pharmacokinetic, DFT modeling, molecular docking, and molecular dynamics simulation approaches: diptoindonesin a as a potential inhibitor of sirtuin-1. *Engineered Science*, *21*, 1–16. https://doi.org/10.30919/es8d794

Agustina, L., & Kasmui. (2021). Studi komputasi aktivitas senyawa turunan santon sebagai antikanker leukemia myeloid kronik K562. *Indonesian Journal of Mathematics and Natural Sciences*, *44*(1), 1–11. https://doi.org/10.15294/ijmns.v44i1.32702

Akrom, M. (2022). Investigasi DFT pada ekstrak tanaman cengkeh dan tembakau sebagai inhibitor korosi hijau. *Jurnal Ilmu Pengetahuan Dan Teknologi*, *33*(1), 1–12.

Akrom, M., & Sutojo, T. (2023). Investigasi model machine learning berbasis QSPR pada inhibitor korosi pirimidin. *Jurnal Ilmiah Teknik Kimia*, *20*(2), 107. https://doi.org/10.31315/e.v20i2.9864

Al-Radadi, N. S., & Abu-Dief, A. M. (2024). Silver nanoparticles (AgNPs) as a metal nano-therapy: Possible mechanisms of antiviral action against COVID-19. *Inorganic and Nano-Metal Chemistry*, *54*(8), 709–727. https://doi.org/10.1080/24701556.2022.2068585

Arain, M., Nafady, A., Haq, M. A. U., Asif, H. M., Ahmad, H. B., Soomro, R. A., Shah, M. R., Mujeeb-Ur-Rehman, & Sirajuddin. (2024). Secnidazole functionalized silver nanoparticles as trace level colorimetric sensor for the detection of cadmium ions. *Optik*, *299*(January), 1–11. https://doi.org/10.1016/j.ijleo.2024.171620

Ashokkumar, K., Simal-Gandara, J., Murugan, M., Dhanya, M. K., & Pandian, A. (2022). Nutmeg (*Myristica fragrans* Houtt.) essential oil: A review on its composition, biological, and pharmacological activities. *Phytotherapy Research*, *36*(7), 2839–2851. https://doi.org/10.1002/ptr.7491

Aziz, D. M., Amin, A. A. M., Hassan, S. A., Özmen, H., Incili, G. K., & Say, Y. (2025). One-pot synthesis of quercetin-functionalized silver and copper nanoparticles for enhanced optical, antimicrobial, and computational properties. *Scientific Reports*, *15*(1), 26391. https://doi.org/10.1038/s41598-025-12586-3

Baskaran, L., Soundarya, V., Gokul, M., Manivannan, S., Ranjith, R., Kumar, P., & Karmegam, N. (2024). Antimicrobial, anticancer and photocatalytic dye degradation activities of silver nanoparticles phytosynthesized from *Secamone emetica* aqueous leaf extract. *Inorganic Chemistry Communications*, *170*(September). https://doi.org/10.1016/j.inoche.2024.113336

Batish, S., & Rajput, J. K. (2023). Quercetin capped silver nanoparticles as an electrochemical sensor for ultrasensitive detection of chloramphenicol in food and water samples. *Journal of Food Composition and Analysis*, *122*(November 2022). https://doi.org/10.1016/j.jfca.2023.105421

Chatterjee, S., Afzal, M., Mandal, P. C., Modak, R., Guin, M., & Konar, S. (2024). Exploration of supramolecular interactions, Hirshfeld surface, FMO, molecular electrostatic potential (MEP) analyses of pyrazole based Zn(II) complex. *Journal of the Indian Chemical Society*, *101*(10). https://doi.org/10.1016/j.jics.2024.101275

Chen, X., Li, H., Qiao, X., Jiang, T., Fu, X., & He, Y. (2021). Agarose oligasaccharide-silver nanoparticle antimicrobial peptide composite for wound dressing. *Carbohydrate Polymers*, *269*(May).

Dhifet, M., Hayder, M., Bezerroug, N., Ghalla, H., Rigane, G., & Salem, R. Ben. (2025). New bis-azido iron(III) meso-arylporphyrin complex: spectroscopic characterization, solid state molecular structure, DFT, MEP, QTAIM calculations and Hirshfeld surface analyses. *Structural Chemistry*.

Dutta, T., Maity, A., Khan, A. A., & Ghosh, N. N. (2024). Activity of pure flavonoid-based green

silver nano particles against breast cancer: A combined experimental and computational investigation. *Journal of Molecular Structure*, *1311*, 138348. https://doi.org/10.1016/j.molstruc.2024.138348

Elfia, H. Y., & Susilo, S. (2023). An update on the pharmacology, phytochemistry, and toxicity of Myristica fragrans Houtt. as a source of treatment: A scoping review. *Journal of Applied Pharmaceutical Science*, *13*(10), 92–106. https://doi.org/10.7324/JAPS.2023.137812

Evita, I. D., Banon, C., S, S. Y., & Adfa, M. (2022). Optimasi hubungan kuantitatif struktur senyawa turunan quercetin yang berpotensi terhadap aktivitas antivirus dengue dengan metode austin model 1 (Optimization of the quantitative relationship between the structure of quercetin derivative compounds that have the potential for dengue antiviral activity using the Austin Model 1 method). *Chimica et Natura Acta*, *10*(2), 53–59. https://doi.org/10.24198/cna.v10.n2.39530

Girma, A., Alamnie, G., Bekele, T., Mebratie, G., Mekuye, B., Abera, B., Workineh, D., Tabor, A., & Jufar, D. (2024). Green-synthesised silver nanoparticles: Antibacterial activity and alternative mechanisms of action to combat multidrug-resistant bacterial pathogens: A systematic literature review. *Green Chemistry Letters and Reviews*, *17*(1). https://doi.org/10.1080/17518253.2024.2412601

Handayani, N. C., Shafira, P. N., & Fadhilah, S. G. (2021). Potensi Pengembangan agen antibakteri dari senyawa kompleks logam transisi di Indonesia (Potential development of antibacterial agents from transition metal complex compounds in Indonesia). *The Indonesian Green Technology Journal*, *2355–4010*, 9–20. https://doi.org/10.21776/ub.igtj.2021.010.01.02

Heydari, S., & Zaryabi, M. H. (2023). Citrate capped silver nanoparticles as naked-eye colorimetric sensor for sensitive and rapid detection of cysteine in biological and environmental samples. *Optical Materials*, *135*(November 2022), 1–10. https://doi.org/10.1016/j.optmat.2022.113376

Huang, X., Pang, Y., Liu, Y., Zhou, Y., Wang, Z., & Hu, Q. (2016). Green synthesis of silver nanoparticles with high antimicrobial activity and low cytotoxicity using catechol-conjugated chitosan. *RSC Advances*, *6*(69), 64357–64363. https://doi.org/10.1039/C6RA09035D

Hussain, R., Saeed, M., Mehboob, M. Y., Khan, S. U., Usman Khan, M., Adnan, M., Ahmed, M., Iqbal, J., & Ayub, K. (2020). Density functional theory study of palladium cluster adsorption on a graphene support. *RSC Advances*, *10*(35), 20595–20607. https://doi.org/10.1039/d0ra01059f

Juma, M. W., Birech, Z., Mwenze, N. M., Ondieki, A. M., Maaza, M., & Mokhotjwa, S. D. (2024). Localized surface plasmon resonance sensing of Trenbolone acetate dopant using silver nanoparticles. *Scientific Reports*, *14*(1), 1–13. https://doi.org/10.1038/s41598-024-56456-w

Kaur, H., Kaur, H., & Sharma, A. (2020). Study of SPR peak shifting of silver nanoparticles with change in surrounding medium. *Materials Today: Proceedings*, *37*(Part 2), 3574–3576. https://doi.org/10.1016/j.matpr.2020.09.584

Khan, R., Akter, M., Kamaraj, C., Malafaia, G., Ragavendran, C., & Rahman, M. (2023). Environmental nanotechnology , monitoring & management green synthesis of silver nanoparticles with its bioactivity , toxicity and environmental applications : A comprehensive literature review. *Environmental Nanotechnology, Monitoring & Management*, *20*(August), 1–17.

Liu, Y., Sun, M., Zhou, Z., Luo, D., Xu, G., & Xiong, Z. (2024). β-CD@AgNPs with peroxisase-like activity for colorimetric determination of chiral tryptophan. *Spectrochimica Acta Part A: Molecular and Biomolecular Spectroscopy*, *323*, 124871. https://doi.org/10.1016/j.saa.2024.124871

Marni, L. G., Emriadi, Syukri, & Imelda. (2022). Mempelajari inhibisi korosi senyawa khellin dan visnagin pada atom besi menggunakan metode DFT (density functional theory) Study (Studying the corrosion inhibition of khellin and visnagin compounds on iron atoms using the DFT (density functional theory) method). *Jurnal Litbang Industri*, *2014*(2), 73–81.

Mikhailova, E. O. (2020). Silver nanoparticles: mechanism of action and probable bio-application. *Journal of Functional Biomaterials*, *11*(4). https://doi.org/10.3390/jfb11040084

Mosallam, F. M., Helmy, E. A., Bendary, M. M., & El-Batal, A. I. (2021). Potency of a novel synthesized Ag-eugenol nanoemulsion for treating some bacterial and fungal pathogens. *Journal of Materials Research*, *36*(7), 1524–1537. https://doi.org/10.1557/s43578-021-00226-1

Ojha, J. K., Ramesh, G., & Reddy, B. V. (2023). Structure, chemical reactivity, NBO, MEP analysis and thermodynamic parameters of pentamethyl benzene using DFT study. *Chemical Physics Impact*, *7*(June), 100280. https://doi.org/10.1016/j.chphi.2023.100280

Padmavathi, J., Udhayakumar, G., Suja, R., Kannaki, K., Sreenathkumar, C., & Gokulakumar, B. (2024). An investigation of silver nanoparticles made from plectranthus amboinicus leaves and their antibacterial and photocatalytic activities. *Journal of the Indian Chemical Society*,

101(10), 101252. https://doi.org/10.1016/j.jics.2024.101252

Pranowo, H. D., Mulya, F., Aziz, H. A., & Santoso, G. A. (2018). Study of substituent effect on properties of platinum(II) porphyrin semiconductor using density functional theory. *Indonesian Journal of Chemistry*, *18*(4), 742. https://doi.org/10.22146/ijc.26121

Putro, P. A., Wulandari, D., Wulandari, D. P., Nurfaidah, F., Ahdan, M. F., Chaerunnisa, S., & Octaviani, V. U. (2024). *Pendekatan simulasi medan gaya untuk menganalisa stabilitas struktur molekuler cyanidin-3-glucoside menggunakan avogadro : Studi pendahuluan* (A force field simulation approach to analyze the stability of the molecular structure of cyanidin-3-glucoside using Avogadro: A preliminary study). *2*(2), 66–76. https://doi.org/10.11594/ timeinphys.2024.v2i2p66-76

Qubtia, M., Ghumman, S. A., Noreen, S., Hameed, H., Noureen, S., Kausar, R., Irfan, A., Akhtar Shah, P., Afzal, H., Hameed, M., Raish, M., Rana, M., Ahmad, A., Kotwica-Mojzych, K., & Bin Jardan, Y. A. (2024). Evaluation of Plant-based silver nanoparticles for antioxidant activity and promising wound-healing applications. *ACS Omega*, *9*(10), 12146–12157. https://doi.org/10.1021/acsomega.3c10489

Rahmah, S. T., & Hartati. (2023). Dampak Nanopartikel Perak Terhadap Pertumbuhan Akar Pada Tanaman Hortikultura (Respon Impact Of Silver Nanoparticles On Root Growth Response In Horticultural Crops). *Prosiding Seminar Nasional Biologi: Inovasi Sains & Pembelajarannya*, *11*, 283–290.

Raj, A., Mandal, J., & Kumari, P. B. (2020). Organo-metallic complex and its implications. *Journal of Pharmacognosy and Phytochemistry*, *9*(2), 491–500. https://doi.org/10.22271/phyto.2020.v9.i2i.10904

Rakhman, K. A., Saraha, A. R., Zainuddin, R., & Abdjan, M. I. (2020). Anthocyanin in flacourtia inermis peel: Analysis and electronic transition study. *Asian Journal of Chemistry*, *32*(1), 941–944.

Rakhman, K. A., Zam Zam, Z., Umar, S., & Abdjan, M. İ. (2020). Study of electronic transition of complex Fe (III), Ni (II) and Zn (II)-1.10-phenanthroline: Modelling and UV-Vis spectra analysis. *Journal of the Turkish Chemical Society Section A: Chemistry*, *7*(1), 155–168. https://doi.org/10.18596/jotcsa.589848

Sakr, M. A. S., Sherbiny, F. F., & El-Etrawy, A. A. S. (2022). Hydrazone-based materials; DFT, TD-DFT, NBO analysis, fukui function, MESP analysis, and solar cell applications. *Journal of Fluorescence*, *32*(5), 1857–1871. https://doi.org/10.1007/s10895-022-03000-6

Shaban, S. M., Taha, A. A., Elged, A. H., Taha, S. T., Sabet, V. M., Kim, D.-H., & Moustafa, A. H. E. (2024). Insights on Gemini cationic surfactants influence AgNPs synthesis: Controlling catalytic and antimicrobial activity. *Journal of Molecular Liquids*, *397*, 124071. https://doi.org/10.1016/j.molliq.2024.124071

Shafi, Z., Pandey, V. K., Habiba, U., Singh, R., Shahid, M., Rustagi, S., Kovács, B., & Shaikh, A. M. (2025). Exploring the food safety and preservation landscape of *Myristica fragrans* (L.) against foodborne pathogen: A review of current knowledge. *Journal of Agriculture and Food Research*, *19*(September 2024). https://doi.org/10.1016/j.jafr.2025.101639

Siegers, B. R. J., Astuty, E., & Taihuttu, Y. M. J. (2022). Uji antibakteri ekstrak etanol daging buah pala (*Myristica fragrans* Houtt.) terhadap bakteri *Staphylococcus aureus* dan *Escherichia coli* (Antibacterial test of ethanol extract of nutmeg fruit flesh (*Myristica fragrans* Houtt.) against *Staphylococcus aureus* and *Escherichia coli* bacteria). *PAMERI: Pattimura Medical Review*, *4*(1), 45–52. https://doi.org/10.30598/pamerivol4 issue1page36-43

Silfadani, L. H., Fakih, T. M., & Wisnuwardhani, H. A. (2022). Desain biosensor berbasis nanopartikel perak untuk deteksi protein hemoglobin pada babi secara in silico (Design of a silver nanoparticle-based biosensor for in silico detection of hemoglobin protein in pigs). *Bandung Conference Series: Pharmacy*, *2*(2). https://doi.org/10.29313/bcsp.v2i2.4697

Sururi, A. M., Sururi, A. M., & Constanty, I. C. (2025). Bioactive compounds of n-hexane fraction of *Syzygium samarangense* stem bark and molecular docking study as anticancer agent. *Jurnal Molekul*, *20*(1), 21–29.

Thomas, T., & Thalla, A. K. (2023). Synthesis of silver nanoparticles using *Myristica fragrans* seed shell: Assessment of antibacterial, antioxidant properties and photocatalytic degradation of dyes. *Journal of Environmental Chemical Engineering*, *11*(2). https://doi.org/10.1016/j.jece.2023.109585

Trung, T. T., Huong, N. T. T., Loc, T. D., Si, N. T., Khuong, V. Q., & Nguyen, P. T. N. (2023). Biogenic one-step synthesis of silver nanoparticles using *Quisqualis indica* linn flower extract: Characterization, molecular docking, and DFT studies. *Inorganic Chemistry Communications*, *158*, 111469. https://doi.org/10.1016/j.inoche.2023.111469

Usman, A., Lobb, K., Pletschke, B. I., Whiteley, C. G., & Wilhelmi, B. S. (2021). Interaction of silver nanoparticles with catechol O-methyltransferase: Spectroscopic and simulation analyses. *Biochemistry and*

Biophysics Reports, *26*, 101013. https://doi.org/10.1016/j.bbrep.2021.101013

Wirwis, A., & Sadowski, Z. (2023). Green Synthesis of silver nanoparticles : Optimizing green tea leaf extraction for enhanced physicochemical properties. *ACS Omega*, *8*, 30532−30549. https://doi.org/10.1021/acsomega.3c03775

Zouaoui, S., Djemoui, B., Mazari, M. M., Miele, M., Pace, V., Houicha, H., Madji, S., Bendeddouche, C. K., Adjdir, M., & Lebouachera, S. E. I. (2025). Clove as a versatile resource: CuO nanoparticles and their catalytic role in eugenol-based triazole synthesis. *Processes*, *13*(8), 2378. https://doi.org/10.3390/pr13082378